Electronic Supporting Information

Nanostructured Copper Sulfide Thin Film *via* a Spatial Successive Ionic Layer Adsorption and Reaction Process Showing Significant Surface-Enhanced Infrared Absorption of CO_2

Yujing Zhang,[a] Xinyuan Chong,[b] Hao Sun,[a] Muaz M. Kedir,[a] Ki-Joong Kim,[c,d] Paul R. Ohodnicki,[c] Alan Wang[b] and Chih-hung Chang*[a]

[a] *School of Chemical, Biological Environmental Engineering, Oregon State University, Corvallis, OR 97331, USA.*
[b] *School of Electrical Engineering and Computer Science, Oregon State University, Corvallis, OR 97331, USA.*
[c] *National Energy Technology Lab, United States Department of Energy, Pittsburgh, PA 15236, USA.*
[d] *LRST, Pittsburgh, PA 15236, USA.*
** Corresponding author. Email address: chih-hung.chang@oregonstate.edu*

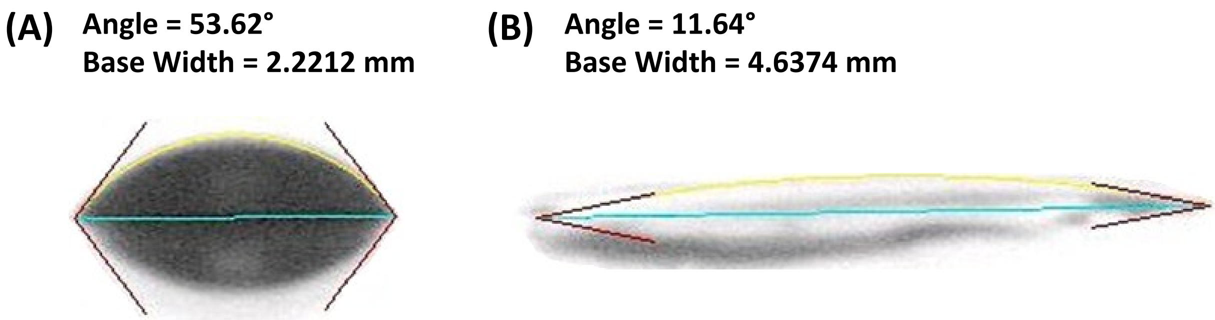

Figure S-1. Contact angles of a bare glass substrate (A) before and (B) after SC-1 of RCA clean.

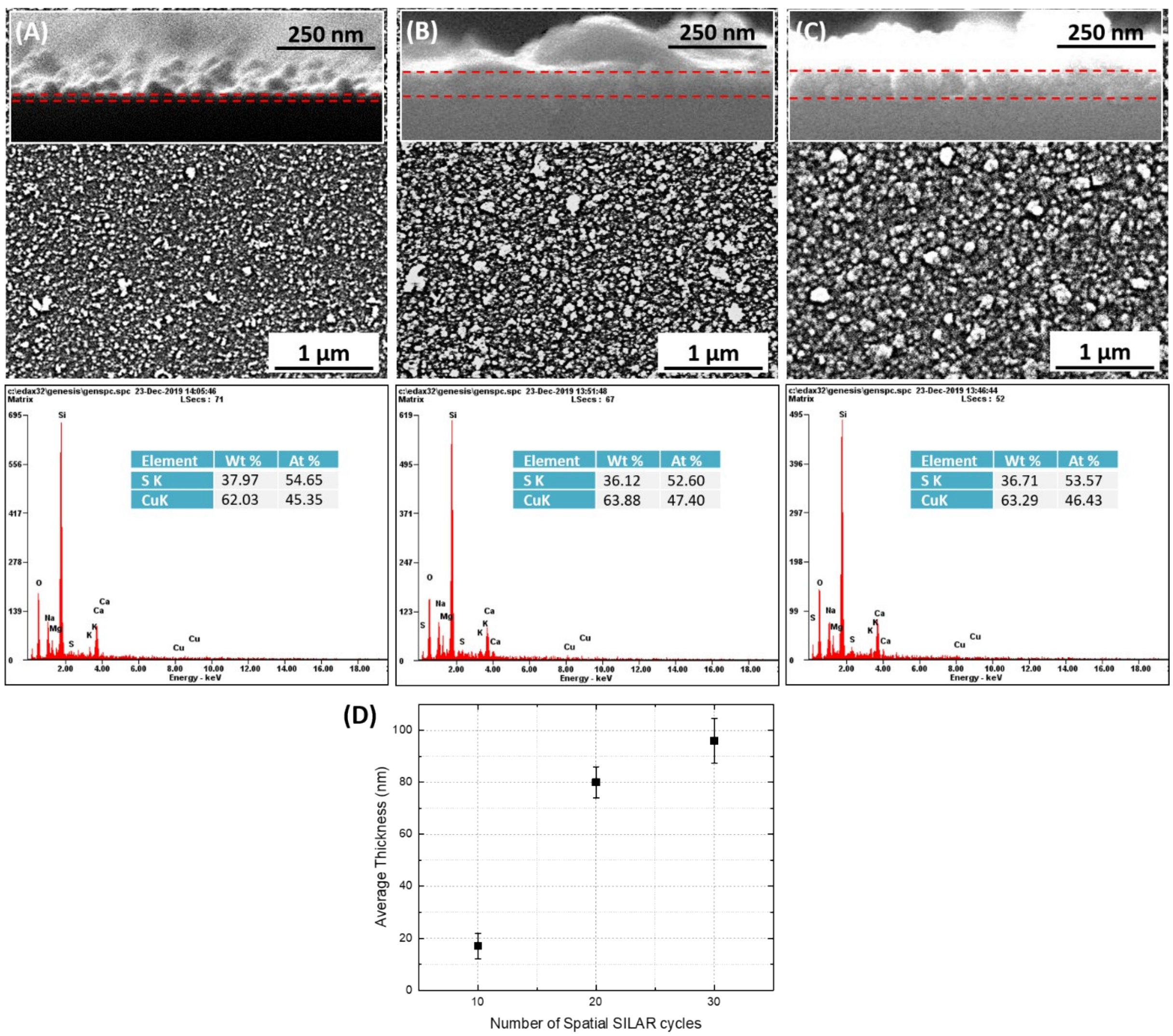

Figure S-2. SEM images (top) and EDX results (bottom) of (A) ***CuS*10**, (B) ***CuS*20**, and (C) ***CuS*30**, inserted are the corresponding cross-section images. (D) The average film thickness as a function of the number of conducted Spatial SILAR cycles.

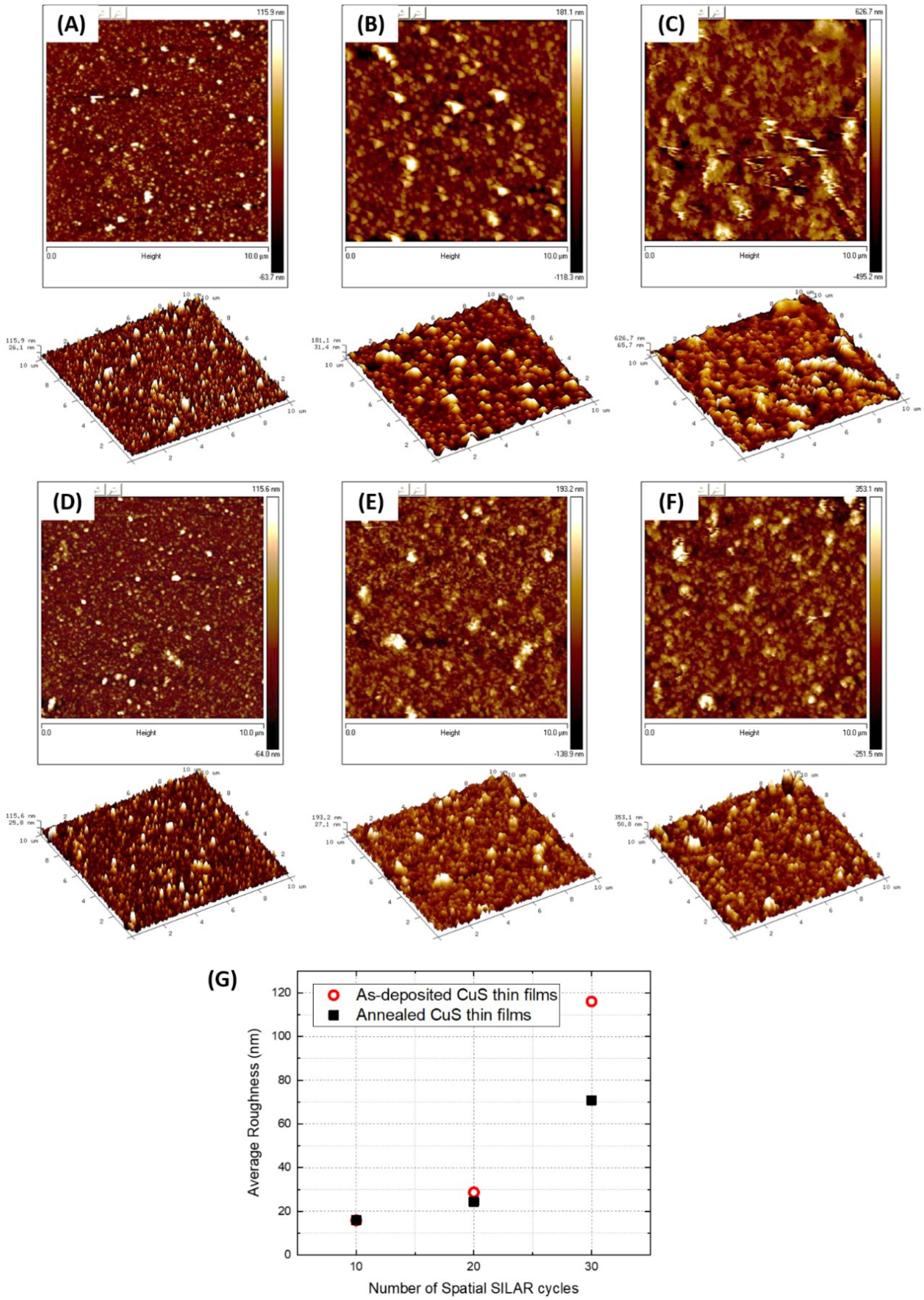

Figure S-3. AFM images of (A-C) as-deposited and (D-F) annealed ***CuS*10**, ***CuS*20**, and ***CuS*30**, respectively. (G) The average film roughness as a function of the number of conducted Spatial SILAR cycles.

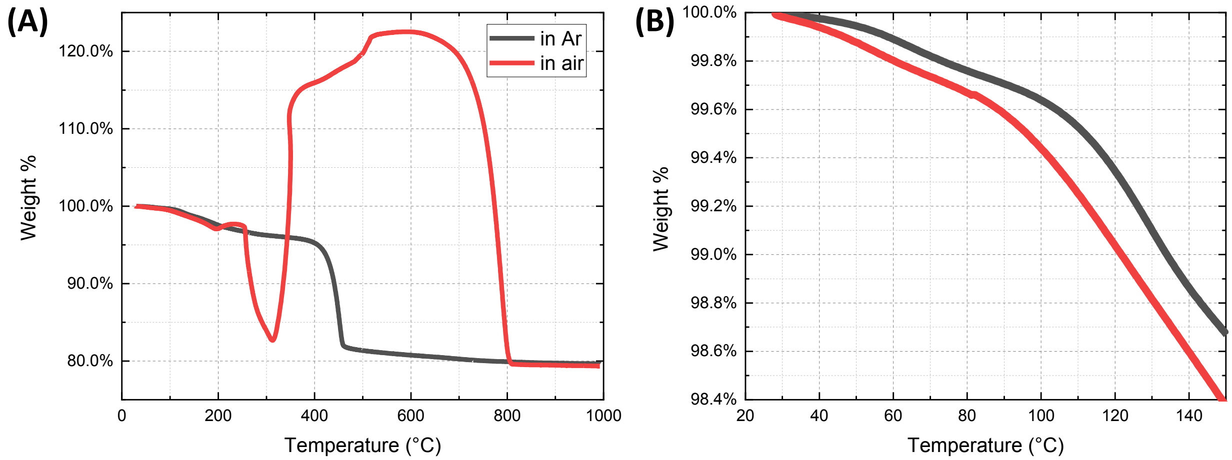

Figure S-4. (A) TGA data of CuS powder prepared by the same precursor solutions as the thin films, and (B) the detailed weight change at low temperature.

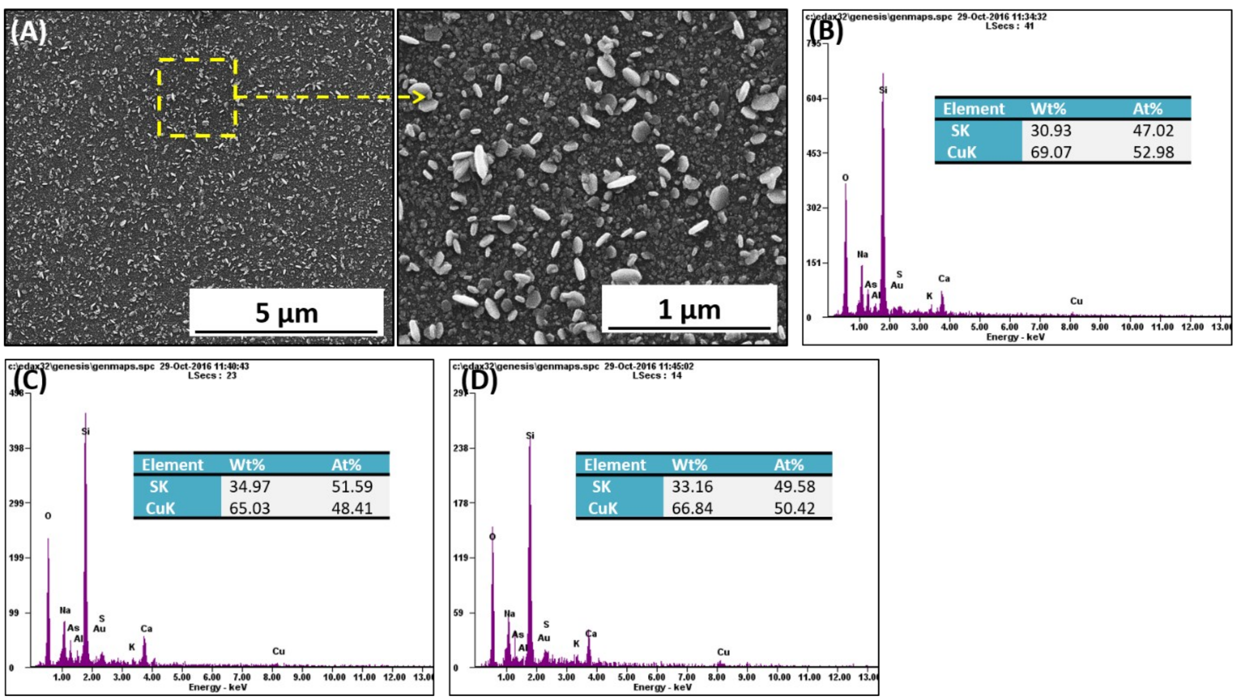

Figure S-5. (A) SEM images of a CuS thin film annealed in air without the cover of silicon wafer under different magnification. The EDX results of (B) a CuS thin film annealed without cover, and a CuS thin film (C) before and (D) after the annealing with cover.

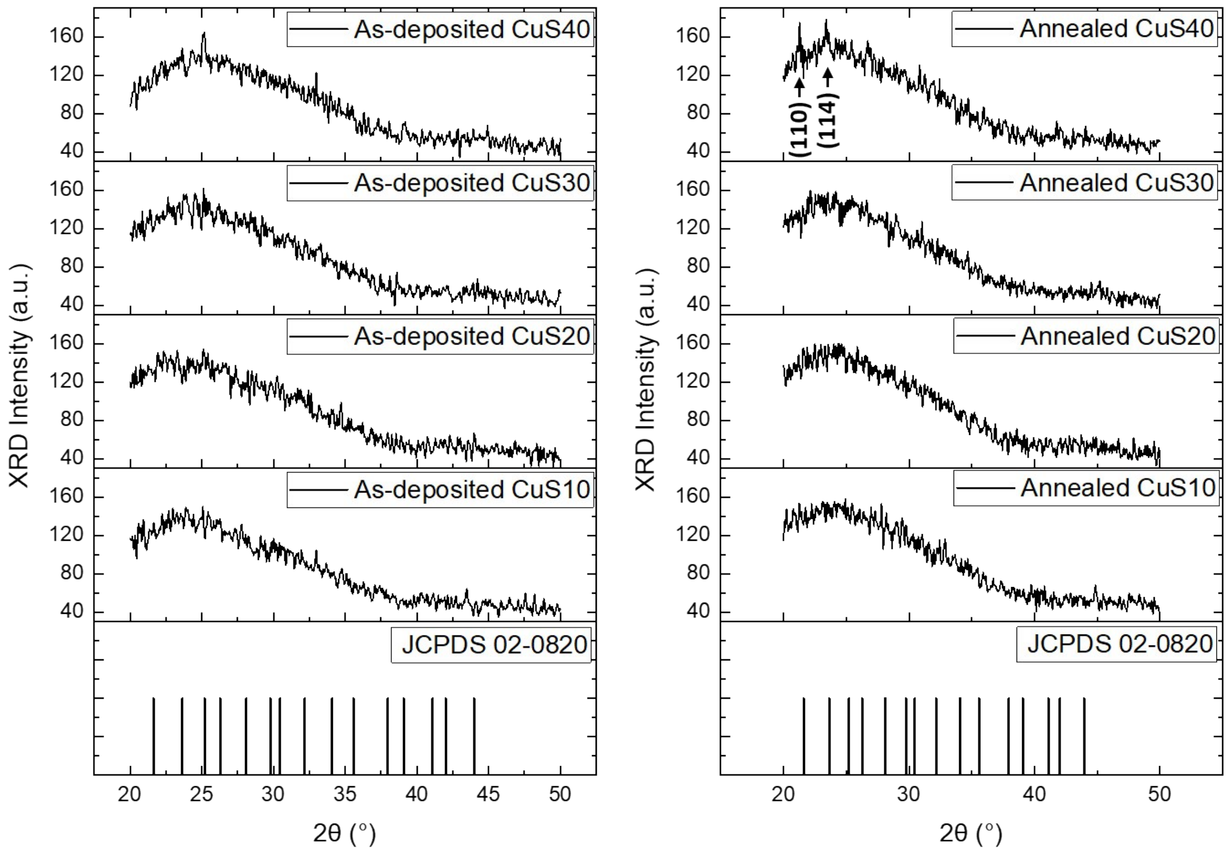

Figure S-6. XRD patterns of (A) as-deposited and (B) annealed CuS thin films.

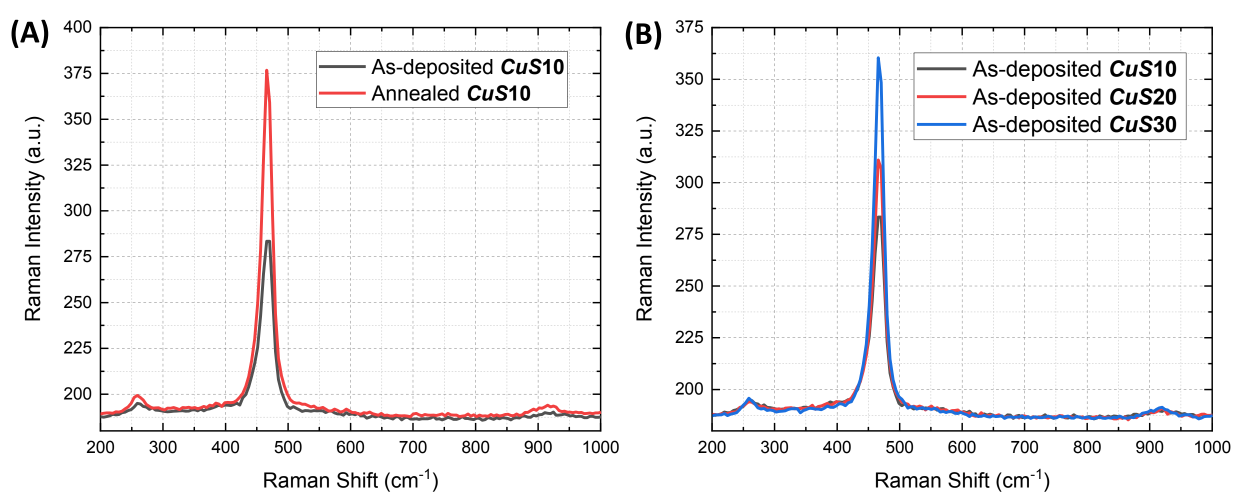

Figure S-7. Raman spectra of (A) ***CuS*10** before and after the low-temperature post-annealing, and (B) CuS thin films deposited with different number of Spatial SILAR cycles.

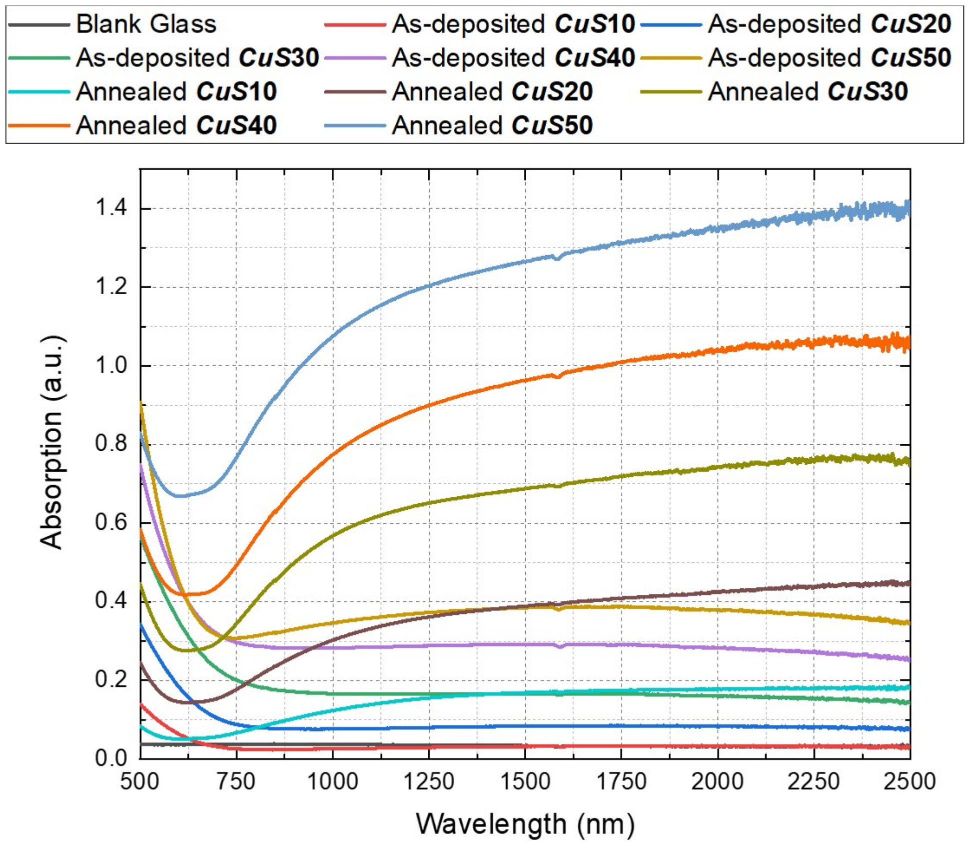

Figure S-8. Vis-NIR absorption spectra of as-deposited and annealed CuS thin films, and a blank glass substrate as a reference for baseline study.

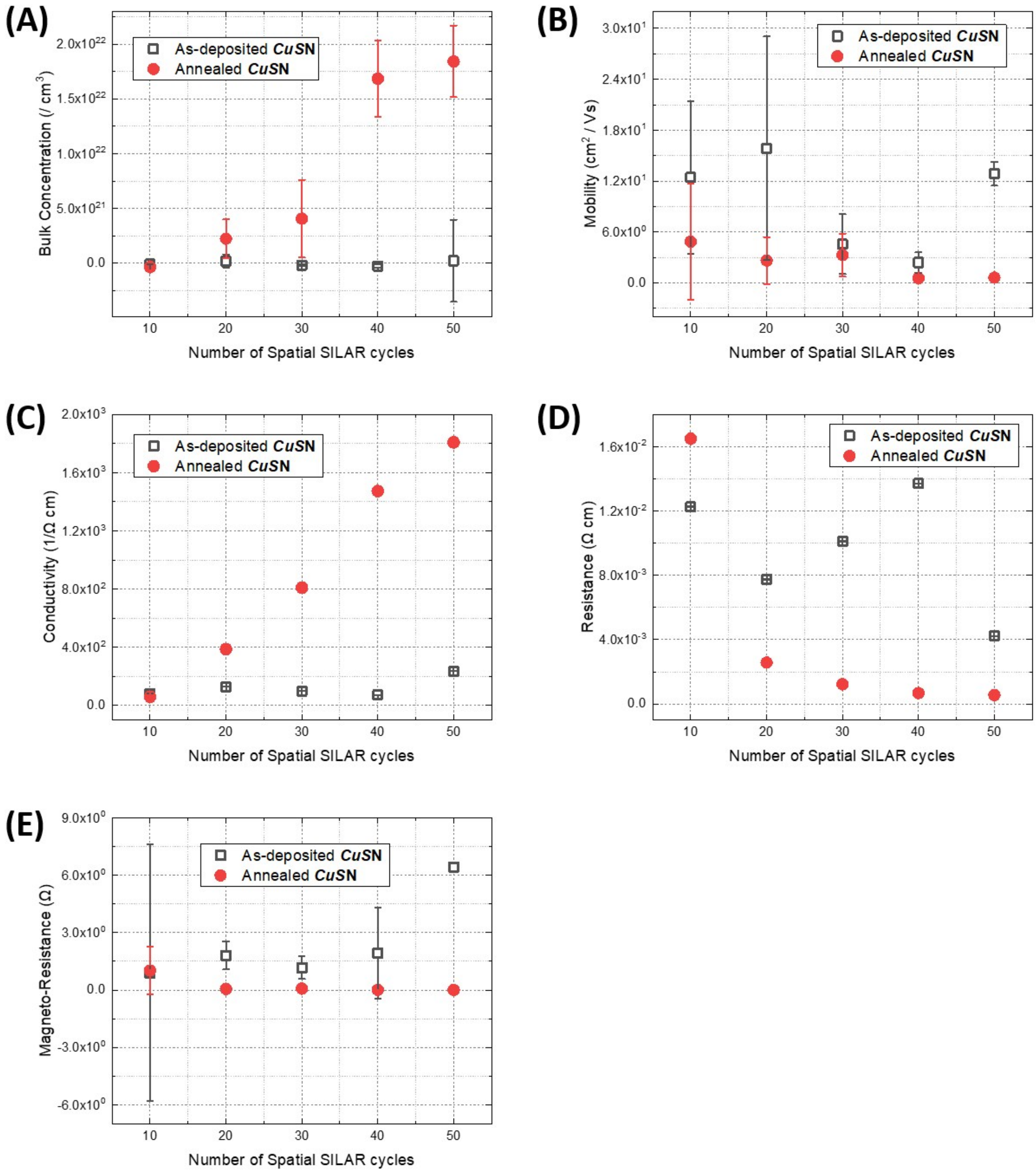

Figure S-9. (A) Average bulk concentration, (B) average mobility, (C) average conductivity, (D) average resistance, and (E) average magneto-resistance of the CuS thin films prepared with different number of Spatial SILAR cycles, measured by Hall Effect Measurement Systems. Hollow and solid symbols represent as-deposited and annealed CuS thin films, respectively.

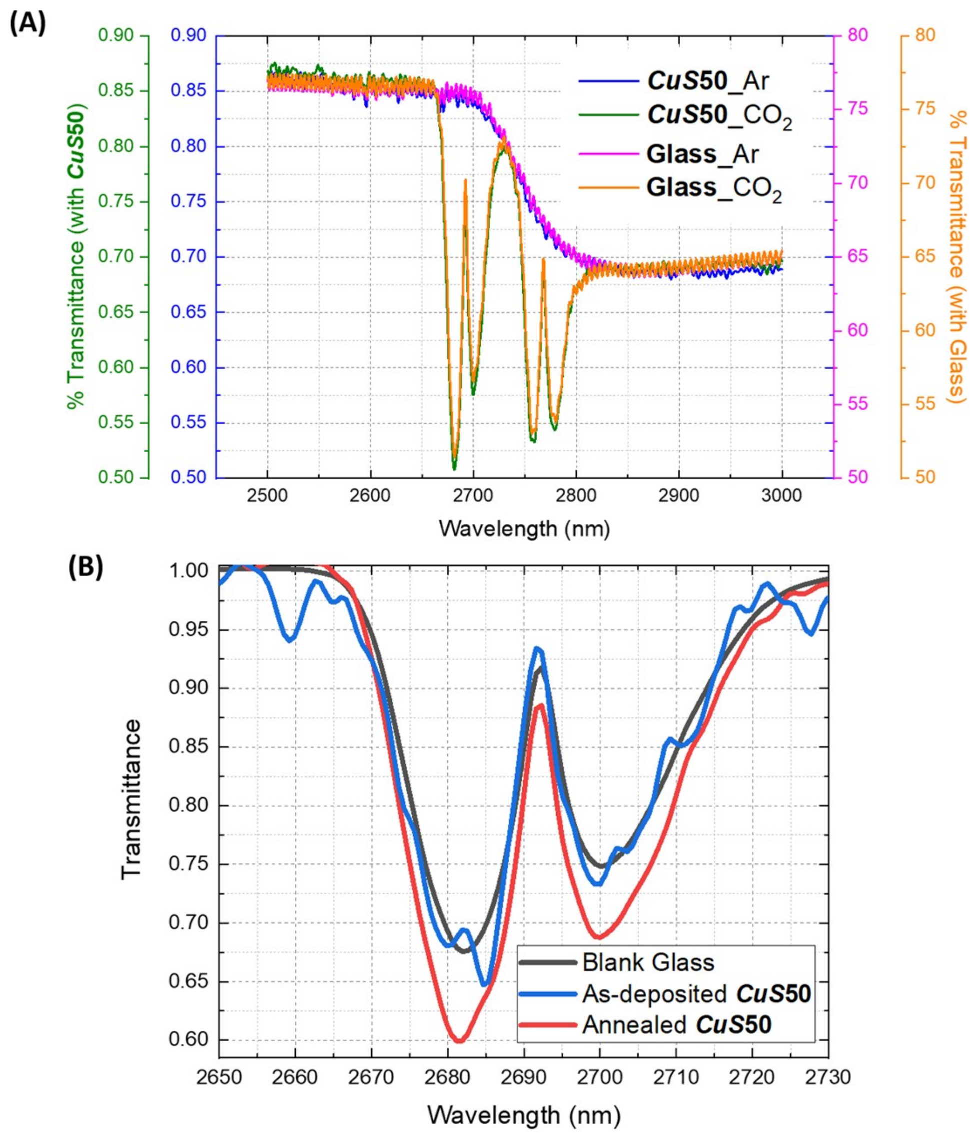

Figure S-10. (A) As-collected FTIR transmission spectra of Ar (100.00%) and CO_2 (100.00%), collected with annealed ***CuS*****50** and a blank glass substrate, respectively. (B) FTIR transmission spectra of CO_2 (100.00%) calculated based on Beer-Lambert Law, originally collected with as-deposited/annealed ***CuS*****50**, and a blank glass substrate for baseline study.

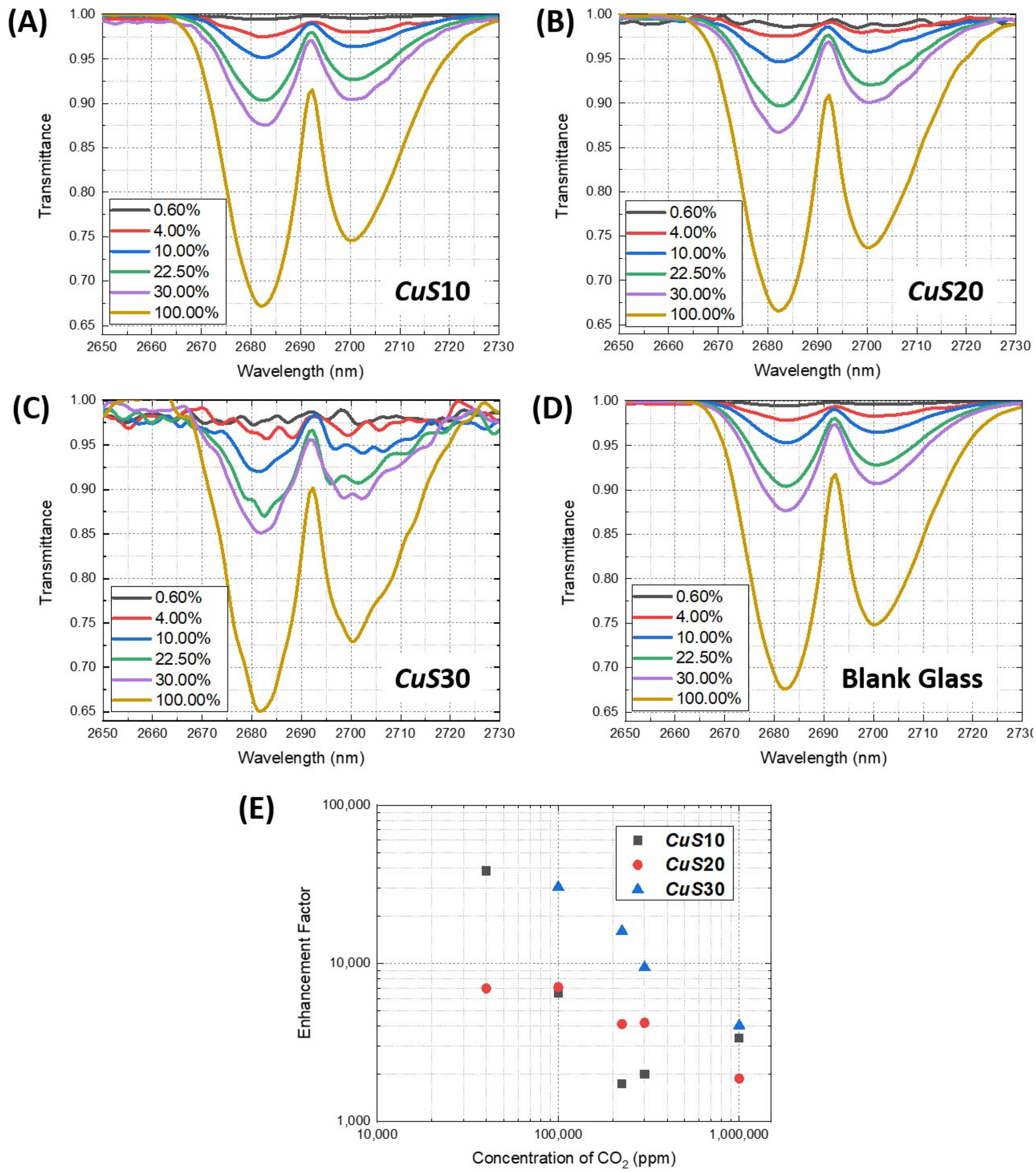

Figure S-11. (A-D) Calculated FTIR transmission spectra of CO_2 with varying concentration, collected with ***CuS*10**, ***CuS*20** or ***CuS*30** integrated with the sensor, and a blank glass substrate as a reference for baseline study. (B) The calculated enhancement factors of these sensors.

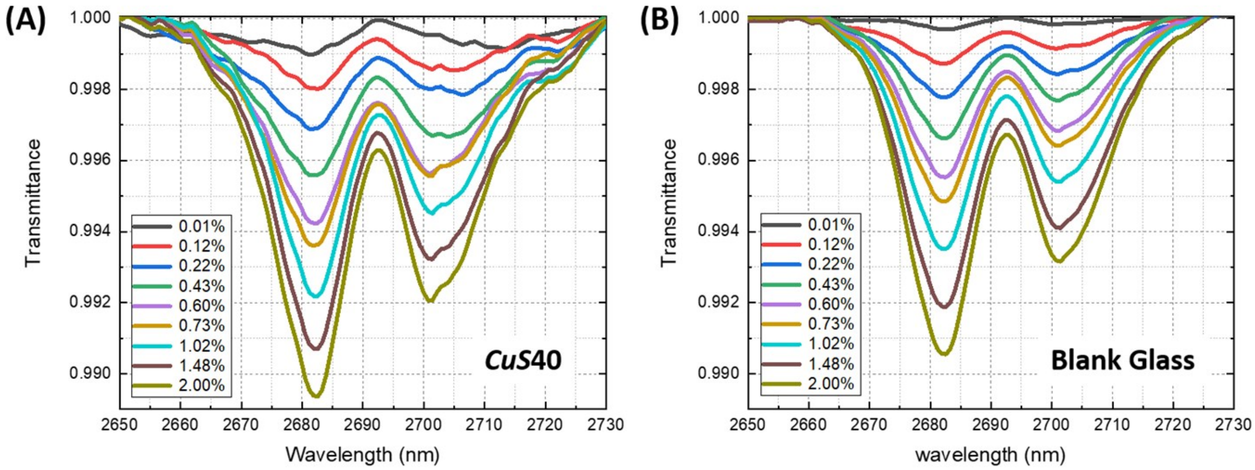

Figure S-12. Calculated FTIR transmission spectra of CO_2 with varying concentration, collected with (A) annealed ***CuS*40** in the sensor, and (B) a blank glass substrate as a reference for baseline study.

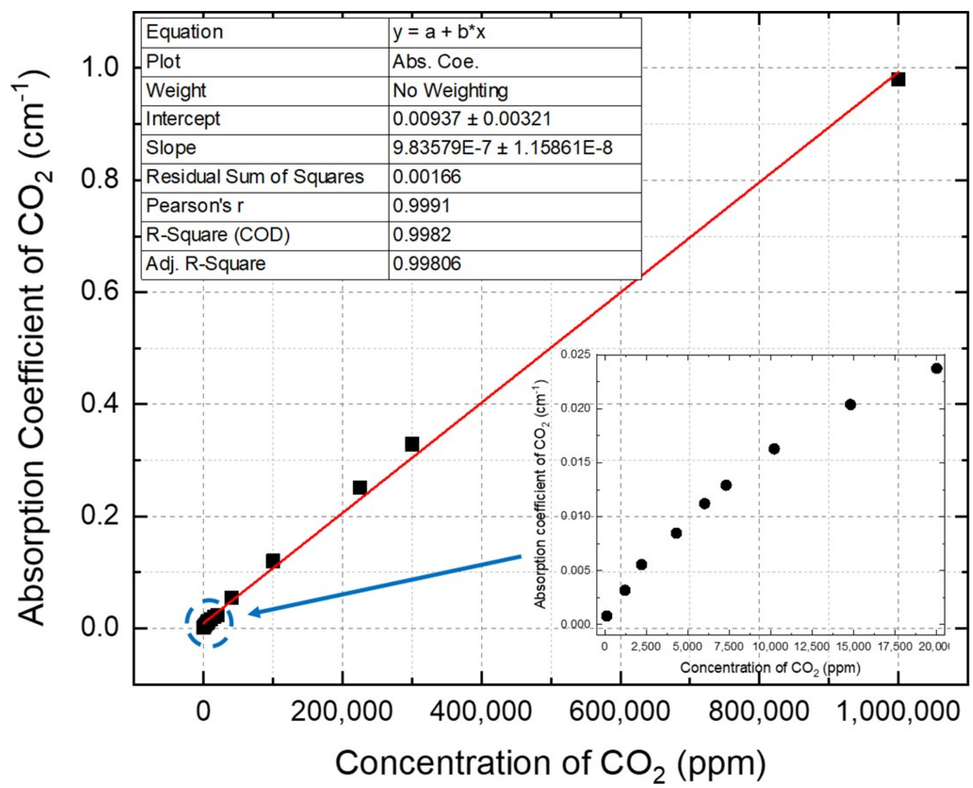

Figure S- 13. Experimental IR absorption coefficient of CO_2 (at approximately 2683 cm^{-1}) as a function of concentration, obtained by the 4-mm gas cell using blank glass substrate and blank sapphire as the optical windows.